Di- and Trimerization of Acetylene over a Model Sn/Pt Catalyst

János Szanyi and Mark T. Paffett*

Contribution from the Chemical Science and Technology Division, MS G740, Los Alamos National Laboratory, Los Alamos, New Mexico 87545

Received May 9, 1994[⊗]

Abstract: The di- and trimerization reactions of acetylene were studied over Pt(111) and ($\sqrt{3}\times\sqrt{3}$)R30°−Sn/Pt-(111) model catalysts at moderate pressures (20−100 Torr, hydrogen−hydrocarbon ratio of 10). The catalyst surfaces were prepared and characterized in a UHV surface analysis system and moderate pressure catalytic reactions were conducted with an attached batch reactor. The overall catalytic activity of the ($\sqrt{3}\times\sqrt{3}$)R30°−Sn/Pt(111) surface alloy was ~4−5 times higher than that of Pt(111). Both surfaces produced only C_4 and C_6 hydrocarbons as di- and trimerization products with C_4 production rates being about an order of magnitude higher than that for C_6 hydrocarbons. Besides the di- and trimerization reaction, hydrogenation of acetylene into ethylene was also observed. Among the C_4 products, butadiene, 1-butene, and *n*-butane were the major components. Both linear and cyclic C_6 hydrocarbons were produced. Among the linear C_6 products paraffinic (*n*-hexane), olefinic (1-hexene), and diolefinic (hexadiene) hydrocarbons were observed. The main components of the cyclic C_6 products were cyclohexane, cyclohexene, 1,3-cyclohexadiene, and benzene. For both product groups the degree of unsaturation of the hydrocarbon molecules depended upon the experimental conditions applied ($P_{H_2}/P_{C_2H_2}$; T). The formation of carbonaceous surface residues was seen under all experimental conditions. The di- and trimerization of acetylene was not eliminated by the presence of surface carbonaceous deposits and even at a high level of carbon buildup the catalysts exhibited significant activities. The very good correlation found between the formation rates of butadiene and cyclic C_6 hydrocarbons suggests that the formation of ring C_6 products proceeds through a metallocyclopentadiene intermediate. This species can either be hydrogenated off from the catalyst surfaces to produce butadiene or be reacted with a third acetylene molecule to form ring C_6 hydrocarbons.

1. Introduction

The exploration of the catalytic chemistry of C_2 hydrocarbons over transition metal catalysts has been the aim of extensive research efforts for several decades. Both homogeneous[1−6] and heterogeneous[7−30] catalytic systems have been studied at length. For the cyclotrimerization reaction of acetylene, Pd was shown to have the highest activity in heterogeneous systems for gas-phase benzene production among the Ni group metals (Ni, Pd, Pt). The other two metals catalyze the decomposition of acetylene with high activities under UHV reaction conditions. In homogeneous catalytic systems Ni-based catalysts have also shown remarkable activities toward benzene formation.[1,2] The production of benzene was observed over other metals as well, for example over Cu.[9] With very few exceptions[18,19,23] all of these studies were carried out under UHV conditions. The only two elevated pressure (>1 Torr) reaction studies we are aware of have been carried out by Rucker et al.[18,19] over single crystal, thin film, and alumina supported Pd catalysts and by Ormerod and Lambert[23] on alumina and titania supported Pd catalysts. Due to the inherent problem of hydrogen absorption into Pd metal these studies were carried out in the absence of gas-phase hydrogen.

The mechanism of the cyclotimerization of acetylene over Pd catalysts has been studied extensively using a wide array of analytical techniques.[12−15,17,20−22,24,25,29] The results of these investigations suggest that the acetylene cyclotrimerization reaction proceeds through a common C_4H_4 intermediate that has metallocyclopentadiene characteristics.[15,21] The formation of benzene through this intermediate is not completely understood and is still debated.[30] The two major routes proposed for benzene formation through this C_4H_4 intermediate are (i)

[⊗] Abstract published in *Advance ACS Abstracts*, January 1, 1995.

(1) Reppe, W.; Schlichting, O.; Klager, K.; Toepal, T. *Justus Liebigs Ann. Chem.* **1948**, *560*, 1.
(2) Schrauzer, G. N.; Glockner, P.; Eichler, S. *Angew. Chem., Int. Ed. Engl.* **1964**, *3(3)*, 185.
(3) Blomquist, A. T.; Maitlis, P. M. *J. Am. Chem. Soc.* **1962**, *84*, 2329.
(4) Maitlis, P. M. *Acc. Chem. Res.* **1977**, *10*, 1.
(5) Parshall, G. W. *Homogeneous Catalysis;* Wiley: New York, 1980.
(6) Vollhardt, K. P. C. *Angew. Chem., Int. Ed. Engl.* **1984**, *23*, 539.
(7) Bryce-Smith, D. *Chem. Ind. (London)* **1964**, 239.
(8) Bertolini, J. C.; Massardier, J.; Dalmai-Imelik, G. J. *J. Chem. Soc., Faraday Trans.* **1978**, *74*, 1.
(9) Avery, N. J. *J. Am. Chem. Soc.* **1985**, *107*, 6711.
(10) Ibach, H.; Lehwald, S. *J. Vac. Sci. Technol.* **1978**, *15(2)*, 407.
(11) Gates, J. A.; Kesmodel, L. L. *J. Chem. Phys.* **1982**, *76(8)*, 428.
(12) Gentle, T. M.; Meutterties, E. *J. Phys. Chem.* **1983**, *87*, 2469.
(13) Gates, J. A.; Kesmodel, L. L. *Surf. Sci.* **1983**, *124*, 68.
(14) Sesselmann, W.; Woratschek, B.; Ertl, G.; Kuppers, J. *Surf. Sci.* **1983**, *130*, 245.
(15) Tysoe, W. T.; Nyberg, G. L.; Lambert, R. M. *Surf. Sci.* **1983**, *135*, 128.
(16) Kesmodel, L. L.; Waddill, G. D.; Gates, J. A. *Surf. Sci.* **1984**, *138*, 464.
(17) Marchon, B. *Surf. Sci.* **1985**, *162*, 382.
(18) Rucker, T. G.; Logan, M. A.; Gentle, T. M.; Muetterties, E. L.; Somorjai, G. A. *J. Phys.Chem.* **1986**, *90*, 2703.
(19) Logan, M. A.; Rucker, T. G.; Gentle, T. M.; Muetterties, E. L.; Somorjai, G. A. *J. Phys.Chem.* **1986**, *90*, 2709.
(20) Patterson, C. H.; Lambert, R. M. *J. Phys. Chem.* **1988**, *92*, 1266.
(21) Patterson, C. H.; Mundenar, J. M.; Timbrell, P. Y.; Gellman, A. J.; Lambert, R. M. *Surf. Sci.* **1989**, *208*, 93.
(22) Hoffmann, H.; Zaera, F.; Ormerod, R. M.; Lambert, R. M.; Wang, L. P.; Tysoe, W. T. *Surf. Sci.* **1990**, *232*, 259.
(23) Ormerod, R. M.; Lambert, R. M. *J. Chem. Soc., Chem. Commun.* **1990**, 1421.
(24) Ormerod, R. M.; Baddeley, C. J.; Lambert, R. M. *Surf. Sci.* **1991**, *259*, L709.
(25) Hoffmann, H.; Zaera, F.; Ormerod, R. M.; Lambert, R. M.; Yao, Y. M.; Saldin, D. K.; Wang, L. P.; Bennett, D. W.; Tysoe, W. T. *Surf. Sci.* **1992**, *268*, 1.
(26) Ormerod, R. M.; Lambert, R. M. *J. Phys. Chem.* **1992**, *96*, 8111.
(27) Xu, C.; Peck J. W.; Koel, B. E. *J. Am. Chem. Soc.* **1993**, *115*, 751.
(28) Hostetler, M. J.; Dubois, L. J. *J. Am. Chem. Soc.* **1993**, *115*, 2044.
(29) Ormerod, R. M.; Lambert, R. M.; Hoffmann, H.; Zaera, F.; Wang, L. P.; Bennett, D. P.; Tysoe, W. T. *J. Phys. Chem.* **1994**, *98*, 2134.
(30) Pacchioni, G.; Lambert, R. M. *Surf. Sci.* **1994**, *304*, 208.

0002-7863/95/1517-1034$09.00/0

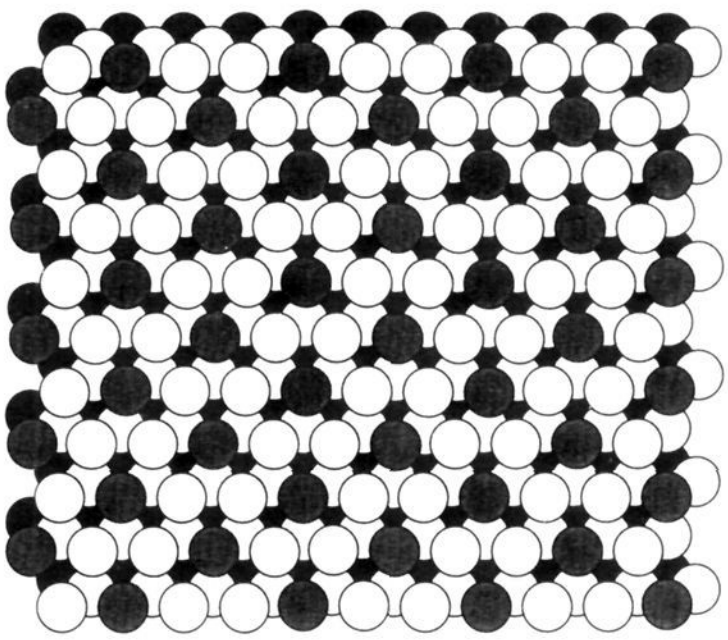

Figure 1. Structure of the $(\sqrt{3}\times\sqrt{3})$R30°−Sn/Pt(111) surface alloy. In the outermost plane the light spheres represent Pt atoms and the dark shaded spheres represent Sn atoms.

addition of a third acetylene molecule or (ii) a two-step reaction which involves the dimerization of C_4H_4 to form a cyclooctatetraene molecule which then decomposes into benzene and acetylene.[30] A recent theoretical study[30] shows that both reaction pathways are energetically feasible although the first reaction route is preferred by the authors. Clearly, the demanding steric and geometric constraints of the adsorbed surface intermediates would suggest a marked surface sensitivity for this reaction. In fact, UHV studies on Pd(111) show superior activity in this reaction over the other two low-index crystal faces. At elevated pressure no difference was seen in cyclotrimerization activities of (111) and (100) Pd surfaces while the (110) face exhibited a much lower benzene formation rate.[18]

In a recent publication Xu et al.[27] reported UHV results which suggest that high acetylene cyclotrimerization activities might be possible for the Sn/Pt(111) surface alloys. The structure of the $(\sqrt{3}\times\sqrt{3})$R30°−Sn/Pt(111) surface alloy is shown in Figure 1. In their UHV study they observed that the decomposition of acetylene was greatly suppressed in reactions conducted at this surface alloy of Sn/Pt(111). Their thermal desorption mass spectroscopic (TDMS) experiments demonstrated very little benzene and no butadiene production over clean Pt(111). On this surface the dominating reaction pathway was the complete decomposition of acetylene into surface carbon and hydrogen. The addition of $\Theta_{Sn} = 0.25$ monolayer (ML) to the Pt(111) surface, which was sufficient to produce the p(2×2)−Sn/Pt-(111) surface alloy, greatly reduced the rate of decomposition of acetylene and produced benzene and with some small unquantified amount of butadiene as well. Acetylene and hydrogen TDMS and post-TDMS AES analysis revealed that the acetylene decomposition channel was almost entirely suppressed at the $\Theta_{Sn} = 0.33$ ML $(\sqrt{3}\times\sqrt{3})$R30°−Sn/Pt(111) surface alloy. This surface showed high activity for benzene formation and the production of butadiene, although the amount of the latter product was not quantified.

It is possible to prepare ordered surface alloys that incorporate Sn into the surface plane of the single crystal template for a number of group VIII transition metals (e.g., Ni, Pd, Pt, Rh, Ru). The alloying of Sn with these transition metals results in very interesting surface and catalytic chemistry.[31−38] For example, the rate of CO oxidation was significantly enhanced at the $\Theta_{Sn} = 0.50$ c(2×2)Sn/Pd(100) surface alloy in comparison to Pd(100).[35] Furthermore, the activity and selectivity patterns were dramatically altered in *n*-butane hydrogenolysis at both the p(2×2) and the $(\sqrt{3}\times\sqrt{3})$R30°−Sn/Pt(111) surface alloys.[37] Our overall motivation has been to prepare and utilize ordered surface alloys that inherently only have certain ensembles (contiguous transition metal atoms) that are available for reaction. This control of catalytic reaction site chemistry has enabled the key fundamentals of catalytic surface science to be implemented in preparing better catalytic surfaces.[35,37] It remains a synthetic challenge to exploit these details in preparing "real world" bimetallic supported transition metal catalysts.

In this paper we report the results of a continuing effort to explore the catalytic properties of these model bimetallic systems. Herein we have conducted catalytic experiments at elevated pressures with an acetylene/hydrogen gas mixture over Pt(111) and $(\sqrt{3}\times\sqrt{3})$R30°−Sn/Pt(111) model catalysts surfaces. Related work on the dimerization and hydrogenolysis reaction chemistry of ethylene/hydrogen mixtures over the same surfaces is presented in another publication.[34] The changes in activity and selectivity are determined for changes in reaction temperature, reactant partial pressure, and reaction time and are all examined in the context of previous UHV characterization studies and prior batch catalytic reaction chemistry.

2. Experimental Section

The experiments were carried out in a combined elevated pressure reactor−UHV surface analysis system which has been described in detail elsewhere.[31,39] Briefly, the UHV chamber is equipped with the basic surface analytical techniques [Auger electron spectroscopy (AES), X-ray photoelectron spectroscopy (XPS), low-energy electron diffraction (LEED), low-energy ion scattering spectroscopy (LEISS), temperature-programmed desorption (TDMS)] and gas and metal dosing facilities. Throughout this study AES was used to determine surface composition and cleanliness prior to and after catalytic experiments. LEED was utilized to verify long-range ordering of the clean substrate metal and the surface alloy. The Pt(111) crystal was mounted on the sample holder rod via tungsten heating wires spot welded to the edge of the crystal. This allowed the heating of the sample up to 1200 K. The crystal temperature was monitored by a chromel/alumel thermocouple spot welded to the edge of the sample. The substrate metal was cleaned with cycles of argon ion sputtering/oxidation/annealing until no impurities were detected by AES. The $(\sqrt{3}\times\sqrt{3})$R30°−Sn/Pt(111) surface alloy was prepared by Sn deposition on the clean Pt(111) substrate metal followed by an anneal to 1000 K. Samples prepared this way gave sharp $(\sqrt{3}\times\sqrt{3})$R30° LEED patterns and its characterization has been given previously in a number of publications.[31,41] The structure of this surface alloy is shown in Figure 1. Activities are given in units of turnover frequency (TOF or the number of product molecules produced per site per second) given relative to the surface atom density of Pt(111), 1.505×10^{15} atoms cm^{-2}. Surface coverages are defined similarly and are given in monolayers (ML). Data obtained at the Sn/Pt(111) surface alloy are presented in terms of the starting Pt(111) surface atom density. A distinction between Sn and Pt atoms has *not* been applied in the reactivity data.

(31) Paffett, M. T.; Windham, R. G. *Surf. Sci.* **1989**, *208*, 34.
(32) Paffett, M. T.; Logan, A. D.; Simonson, R. J.; Koel, B. E. *Surf. Sci.* **1991**, *250*, 123.
(33) Paffett, M. T.; Logan, A. D.; Taylor, T. N. *J. Phys. Chem.* **1993**, *97*, 690.
(34) Szanyi, J.; Paffett, M. T. *Catal. Lett.* **1994**, *29*, 133.
(35) Logan, A. D.; Paffett, M. T. *J. Catal.* **1992**, *133*, 179.
(36) Logan, A. D.; Paffett, M. T. *New Frontiers in Catalysis*; Proceedings of the 10th International Congress on Catalysis, Budapest, Hungary, July 1992; p 1595.
(37) Szanyi, J.; Anderson, S. L.; Paffett, M. T. *J. Catal.* **1994**, *149*, 438.
(38) Anderson, S. L.; Datye, A. K.; Henn, F. C.; Szanyi, J.; Paffett, M. T. *Catal. Lett.*, submitted for publication.
(39) Campbell, C. T.; Paffett, M. T. *Surf. Sci.* **1984**, *139*, 396.
(40) Xu, C.; Koel, B. E.; Paffett, M. T. *Langmuir* **1994**, *10*, 166.
(41) Overbury, S. H.; Mullins, D.; Paffett, M. T.; Koel, B. E. *Surf. Sci.* **1991**, *254*, 45.
(42) Ku, Y.-S.; Overbury, S. H. *Surf. Sci.* **1992**, *273*, 353.

Following sample preparation the catalyst was transferred into the elevated-pressure reaction cell for batch catalytic run measurements. During catalytic experiments the UHV chamber was separated from the reaction cell by a gate valve. The acetylene/hydrogen reactant gas mixture was prepared in situ in the reaction cell. After the introduction of the gases a sufficient amount of time was allowed to ensure complete mixing of the gas components. The sample temperature was then raised rapidly to the desired value and kept at that level for the duration of the catalytic run with a ±2 K precision. After a given reaction time the reaction was quenched by sudden cooling of the catalyst. The reactant/product gas mixture was then condensed into a liquid nitrogen cooled trap and transferred to a gas chromatograph (GC) for analysis. The GC separation was carried out over a Porapack N column operated at 423 K and a flame ionization detector was used for analysis. The catalyst sample was transferred back into the UHV chamber for postreaction surface analysis.[37] Carbon surface coverage is given in monolayers after the calibration procedure of Sachtler and Somorjai.[43] This calibration is at best a qualitative one because of recent STM measurements of Land et al.[44] that demonstrate that conversion of the carbonaceous residue resulting from decomposition of ethylene to graphite results in island growth. Therefore, relative carbon coverage is shown as AES ratios for comparative purposes.

Throughout the catalytic measurements, research purity gases of acetylene and hydrogen were used. Hydrogen was used without further purification. The acetylene was further purified rigorously before use. First it was condensed into a liquid nitrogen cooled glass bulb and pumped for extended periods of time to eliminate methane impurities. In the next step acetylene was passed through an activated, dry ice/acetone cooled zeolite 5 Å trap and condensed into a metal bulb cooled with liquid nitrogen. The metal bulb then was separated from the zeolite trap and the zeolite was reactivated by heating it for about an hour at 523 K. The zeolite trap was then cooled down again with the dry ice/acetone cold bath and the acetylene was passed through it into a clean, liquid nitrogen cooled glass bulb. The acetylene purified by this method contained only a very small amount of methane impurity. Detector sensitivity factors for saturated and monoalkene C_1–C_6 hydrocarbons were determined using calibration gas mixtures (Scott Specialty gases, Nos. 220 and 222). Retention times for other C_4 and C_6 hydrocarbons (primarily linear and cyclic dienes) were determined using research grade liquids available from Aldrich Chemical Co. Rate data are initial rates of conversion with less than 2% reactant consumed per batch reaction and selectivities are given in mole percent.

3. Results

1. Temperature Dependence. The catalytic activities of Pt(111) and $(\sqrt{3}\times\sqrt{3})$R30°–Sn/Pt(111) model catalysts were determined for the acetylene di- and trimerization reactions using a 1:10 acetylene–hydrogen reactant gas mixture at a total pressure of 22.0 Torr over the temperature range of 400–540 K. The catalytic activities expressed as turnover frequencies (TOF) are displayed in Figures 2 and 3 for Pt(111) and $(\sqrt{3}\times\sqrt{3})$R30°–Sn/Pt(111), respectively, in Arrhenius form. The major products detected were C_4 and C_6 hydrocarbons with only trace amounts of methane and propane observed at the highest reaction temperatures studied. The main C_4 products were *n*-butane (C_{4-}), 1-butene ($C_{4=}$), and butadiene. The GC separation and analysis method was not sufficient for the accurate quantification of *n*-butane and 1-butene. No C_3 or C_5 products were seen in any of the catalytic experiments under these reaction conditions. The C_6 products formed in the $C_2H_2 + H_2$ reaction are divided into two groups composed of linear and ring C_6 hydrocarbons. Among the linear C_6 hydrocarbons, saturated, olefinic, and diolefinic molecules were seen in the product gas mixture. The ring C_6 mixture contained cyclohexane, cyclohexene, cyclohexadiene (mostly 1,3), and benzene. The linear and ring C_6 hydrocarbons could be accurately

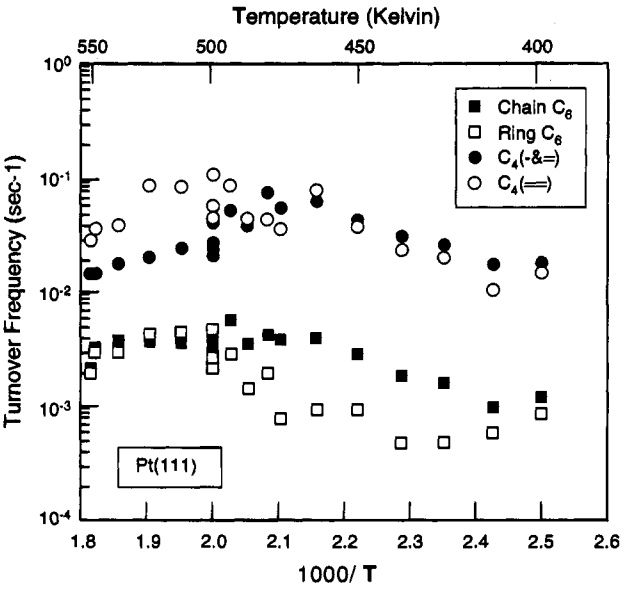

Figure 2. Arrhenius plots for acetylene di- and trimerization products over Pt(111).

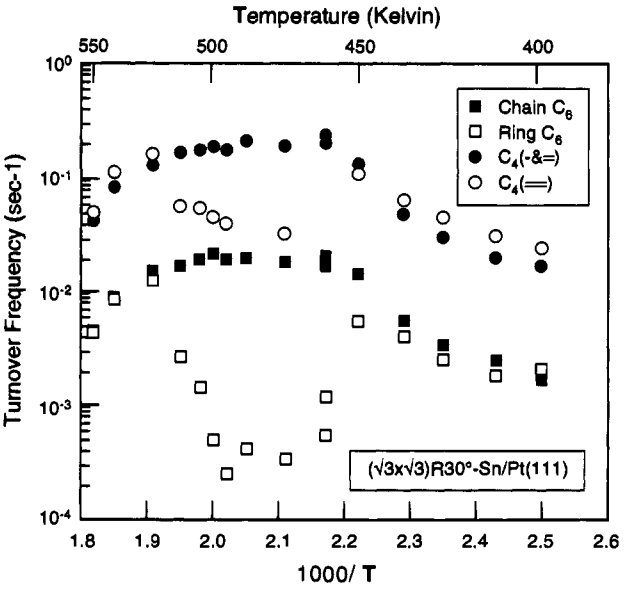

Figure 3. Arrhenius plots for acetylene di- and trimerization products over $(\sqrt{3}\times\sqrt{3})$R30°–Sn/Pt(111) surface alloy.

separated and quantitatively analyzed; therefore, throughout this paper we present them as linear and ring C_6 hydrocarbon products. The temperature dependences of the catalytic activity patterns for all four products displayed on these two model catalysts were very similar; however, at both surfaces the C_4 formation rates were about an order of magnitude higher than the C_6 formation rates (Figures 2 and 3). Over the temperature range 400–470 K the production rate of all hydrocarbons increased monotonically with increasing reaction temperature with the slopes of the initial portions of the Arrhenius plots very close to each other for all products and for both surfaces, except for the ring C_6 production over Pt(111) which is very low in this temperature range. The apparent activation energy evaluated from the slopes of these Arrhenius plots is about 11–12 kcal mol^{-1}. On both surfaces, and particularly over the $(\sqrt{3}\times\sqrt{3})$R30°–Sn/Pt(111) surface alloy, the formation rates of ring C_6 products parallel that of butadiene while the tendency in linear C_6 production rate is very similar to that of the $C_{4(-\&=)}$ in this temperature range. Over Pt(111) at ~480 K the $C_{4(-\&=)}$

(43) Sachtler, W. M. J.; Somorjai, G. A. *J. Catal.* **1983**, *81*, 77.
(44) Land, T. A.; Michely, T.; Behm, R. J.; Hemminger, J. C.; Comsa, G. *J. Chem. Phys.* **1992**, *97*, 6774.

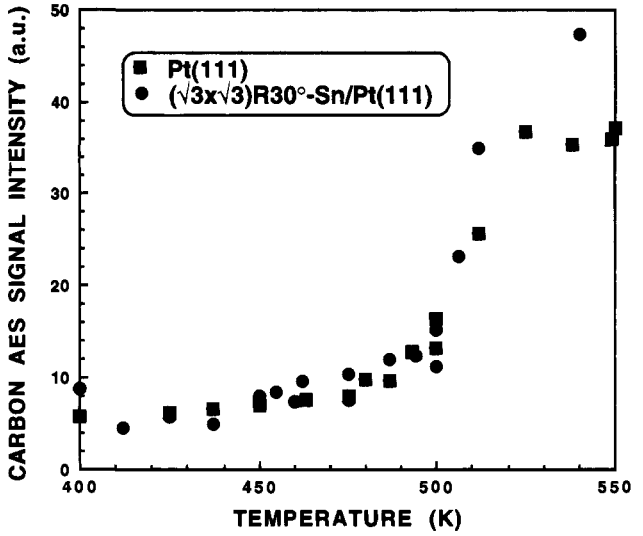

Figure 4. Postreaction carbon coverage (monolayers) on Pt(111) and ($\sqrt{3}\times\sqrt{3}$)R30°−Sn/Pt(111) as a function of reaction temperature during acetylene cyclotrimerization.

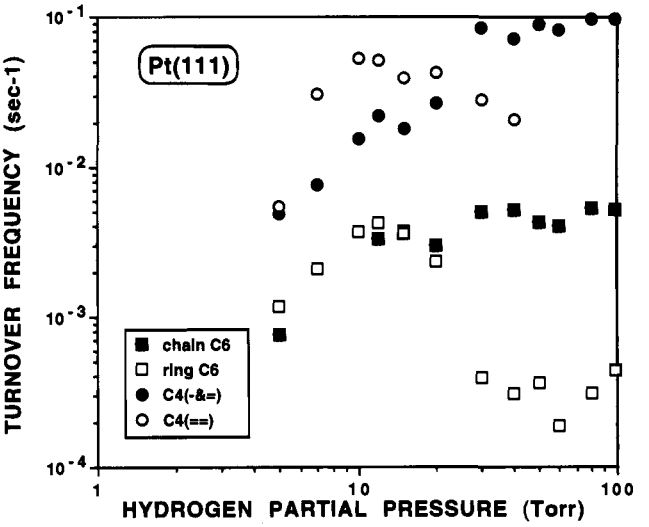

Figure 5. Hydrogen partial pressure dependences of the product formation rates in the di- and trimerization of acetylene over Pt(111).

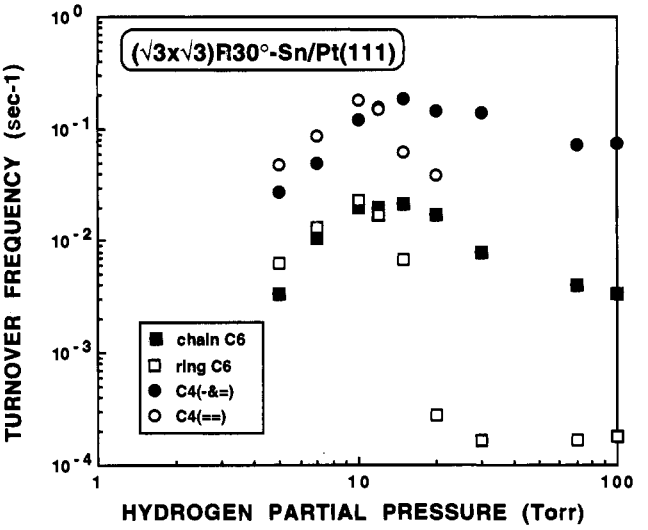

Figure 6. Hydrogen partial pressure dependences of the product formation rates in the di- and trimerization of acetylene over ($\sqrt{3}\times\sqrt{3}$)-R30°−Sn/Pt(111).

and linear C_6 formation rates reach a maximum and their rates fall off as the reaction temperature is increased further. In the 470−500 K temperature range there is a slight drop in butadiene formation rate and at the same time the TOF for ring C_6 production decreases. Above 500 K the specific butadiene formation rates parallel that of $C_{4(-\&=)}$ but at higher values. Concomitantly, the TOFs for ring C_6 formation follow very closely that of linear C_6 formation. Over the ($\sqrt{3}\times\sqrt{3}$)R30°−Sn/Pt(111) surface alloy the same trends in catalytic activities are observed but the decrease in catalytic activity for butadiene and ring C_6 formation is much more pronounced in the 470−510 K temperature range than it is over Pt(111). The activity of the ($\sqrt{3}\times\sqrt{3}$)R30°−Sn/Pt(111) alloy fully recovers above 510 K and the specific reaction rates for butadiene and ring C_6 again follow very closely that of $C_{4(-\&=)}$ and linear C_6, respectively. In the temperature range where decreased production of butadiene and ring C_6 occur the $C_{4(-\&=)}$ and linear C_6 production rates are practically constant. Above 510 K the specific formation rates for all hydrocarbons decrease with increasing reaction temperature.

In addition to following the hydrocarbon production rates over the two catalysts the carbon buildup on the surfaces of the catalysts was monitored by postreaction AES analysis. After a batch catalytic reaction run the sample was cooled in the reaction mixture, transferred back into the UHV chamber, and subsequently flashed to reaction temperature in order to decrease contributions to the 274 eV carbon AES signal from adsorbed hydrocarbon molecules. A certain level of carbon will always be present due to this procedure (0.15−0.2 ML); however, substantial (>0.2 ML) relative carbon buildup can be monitored in this manner. Figure 4 displays the carbon Auger signal intensities as a function of reaction temperature for both Pt(111) and ($\sqrt{3}\times\sqrt{3}$)R30°−Sn/Pt(111). The carbon Auger signal intensities from the two surfaces fall on the same line in the temperature range of 400−500 K. The increase in carbon buildup over this temperature interval is slight and the intensity of the carbon Auger signal approximately doubles at the high-temperature end. This coverage remains relatively low at Θ_c = 0.6 ML (at 500 K) based on the calibration method of Sachtler and Somorjai.[43] A dramatic increase in carbon Auger signal intensity is seen between 500 and 520 K. In this small temperature interval the carbon Auger signal intensity increases by a factor of ~3. Above 520 K the carbon Auger signal intensity remains constant at a high level (Θ_c > 4.0 ML).

2. Hydrogen Partial Pressure Dependence. The hydrogen partial pressure dependencies of the reaction rates for the production of all four hydrocarbons were studied at a constant acetylene pressure of 2.0 Torr at 500 K in the hydrogen pressure range of 5−100 Torr. The total pressure in the reaction cell was kept constant at 102 Torr using neon as the balance gas. The TOFs for all four hydrocarbons as a function of hydrogen partial pressure are plotted in Figures 5 and 6 for Pt(111) and ($\sqrt{3}\times\sqrt{3}$)R30°−Sn/Pt(111), respectively. Over Pt(111) at low hydrogen pressures (5−10 Torr) the formation rates of all four hydrocarbon products are first order in hydrogen pressure. At P_{H_2} = 10 Torr both the butadiene and ring C_6 formation rates reach maxima and roll over at higher hydrogen pressures. The TOF for ring C_6 production is practically unchanged at hydrogen pressures over 30 Torr. The change in butadiene formation rate shows the same characteristics. The TOFs for $C_{4(-\&=)}$ formation increase with hydrogen pressure even after the butadiene production rate has passed through its maximum. Above 30 Torr of hydrogen pressure the $C_{4(-\&=)}$ products are formed with the highest selectivity and their

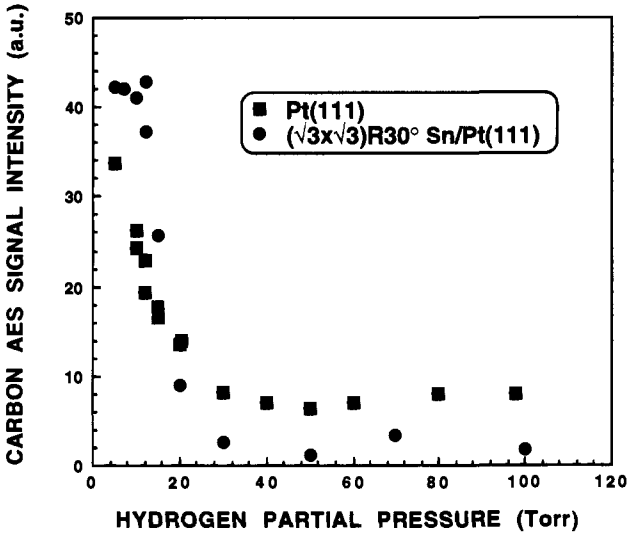

Figure 7. The effect of hydrogen partial pressure on the carbon buildup on Pt(111) and ($\sqrt{3}\times\sqrt{3}$)R30°−Sn/Pt(111) surfaces during acetylene di- and trimerization.

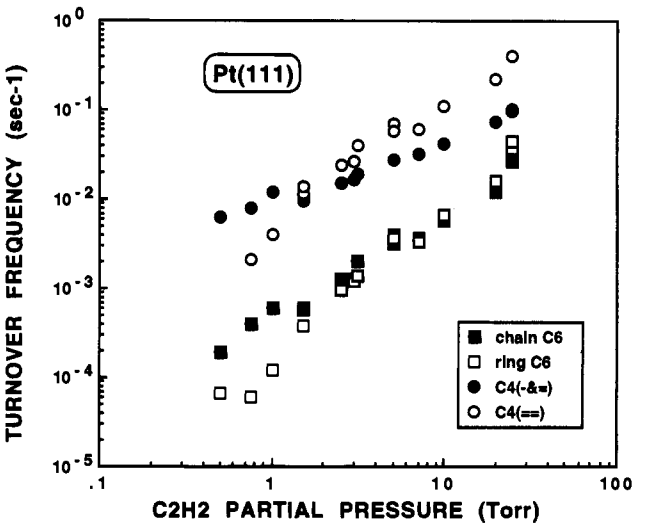

Figure 8. Acetylene partial pressure dependences of the product formation rates in the di- and trimerization of acetylene over Pt(111).

production rates are constant. Very similar behavior is seen for the linear C_6 hydrocarbon formation rates. Their values remain unchanged at hydrogen pressures higher than 30 Torr. The hydrogen partial pressure dependencies of C_4 and C_6 hydrocarbon formation rates over ($\sqrt{3}\times\sqrt{3}$)R30°−Sn/Pt(111) show similar trends to those observed at Pt(111). At low hydrogen pressures (<10 Torr) the TOFs of all C_4 and C_6 hydrocarbons increase with increasing hydrogen pressure with a first-order dependence. In this temperature range butadiene is produced with the highest formation rate, and furthermore, the production rate of ring C_6 hydrocarbons exceeds that of linear C_6 hydrocarbons. At P_{H_2} = 10 Torr both the butadiene and ring C_6 formation rates reach maxima and then they roll over and decrease rapidly with increasing hydrogen partial pressure. The TOFs for ring C_6 formation are constant at P_{H_2} > 30 Torr on the ($\sqrt{3}\times\sqrt{3}$)R30°−Sn/Pt(111) catalyst as also seen for Pt(111). The production rates for $C_{4(-\&=)}$ and linear C_6 hydrocarbons each reach maxima at $P_{H_2} \sim 15$ Torr and thereafter they both decrease. However, the decrease in $C_{4(-\&=)}$ and linear C_6 formation rates are much lower than those seen for butadiene and ring C_6 hydrocarbons. In contrast to Pt(111) at P_{H_2} > 30 Torr where the $C_{4(-\&=)}$ and linear C_6 formation rates were constant, over the ($\sqrt{3}\times\sqrt{3}$)R30°−Sn/Pt(111) surface alloy their formation rates are *negative* order in hydrogen partial pressure. Above 30 Torr of hydrogen pressure, at the ($\sqrt{3}\times\sqrt{3}$)-R30°−Sn/Pt(111) surface alloy and the Pt(111) surface the $C_{4(-\&=)}$ hydrocarbons are the dominant products. Note that over both Pt(111) and ($\sqrt{3}\times\sqrt{3}$)R30°−Sn/Pt(111) surfaces the formation rates of ring C_6 hydrocarbons parallel that of butadiene and the production rates of linear C_6 hydrocarbons parallel closely that of $C_{4(-\&=)}$.

Postreaction carbon Auger signal intensities as a function of hydrogen partial pressure are shown in Figure 7 for both surfaces. The carbon Auger signal intensities at P_{H_2} < 10 Torr over the alloy surface are very high and constant at $\Theta_C \sim 4.0$ ML. On both surfaces the carbon signal intensity decreases rapidly in the 10−20 Torr hydrogen partial pressure range. No changes in carbon Auger signal intensities were seen over either surface at hydrogen pressures over 30 Torr. These signals stay at a comparatively low, constant level of $\Theta_C \sim 0.2$−0.4 ML. The ($\sqrt{3}\times\sqrt{3}$)R30°−Sn/Pt(111) is practically carbon-free above 30 Torr of hydrogen pressure.

3. Acetylene Partial Pressure Dependence. The acetylene partial pressure dependencies of the C_4 and C_6 hydrocarbon formation rates were studied in detail over the Pt(111) surface at 500 K at a constant hydrogen pressure of 20 Torr and at a total pressure of 100 Torr. Neon was used again as a balance gas. The TOFs for all C_4 and C_6 hydrocarbon products as a function of acetylene partial pressure are displayed in Figure 8 for the Pt(111) surface. (The same acetylene pressure dependencies were seen for all hydrocarbon products over the ($\sqrt{3}\times\sqrt{3}$)R30°−Sn/Pt(111) surface alloy as for Pt(111) except that the absolute formation rates were somewhat higher over the surface alloy.) Over the entire acetylene partial pressure range studied (0.5−25.0 Torr) every product formation rate has a positive-order dependence on the partial pressure of acetylene. The $C_{4(-\&=)}$ and linear C_6 formation rates increase monotonically in the whole acetylene pressure interval, although the slopes of the two curves are different. The linear C_6 formation rate has a stronger positive order dependence on acetylene pressure than $C_{4(-\&=)}$ and its value approaches that of $C_{4(-\&=)}$ as the partial pressure of acetylene increases. The changes in butadiene and ring C_6 formation rates again show striking similarities. At low acetylene partial pressures (<1.5 Torr) the TOFs for both products increase sharply with acetylene pressure. At $P_{C_2H_2}$ > 1.5 Torr the increases in butadiene and ring C_6 formation rates are slower than that at $P_{C_2H_2}$ < 1.5 Torr, but their formation rates have stronger positive-order dependences than that seen for either $C_{4(-\&=)}$ or linear C_6 hydrocarbons. The TOFs for ring C_6 formation increase faster than for butadiene, which suggests that the rate of the propagation step from C_4 to C_6 is more drastically influenced by acetylene partial pressure than the initial dimerization step at these higher acetylene pressures.

4. Deactivation. The deactivation of both Pt(111) and ($\sqrt{3}\times\sqrt{3}$)R30°−Sn/Pt(111) catalysts has been followed at 500 K reaction temperature using an 1:10 acetylene−hydrogen reactant gas mixture at a total pressure of 22.0 Torr. The surface of the sample was not cleaned between subsequent catalytic runs. After each reaction experiment the changes in surface composition were determined with AES. The TOFs for all C_4 and C_6 hydrocarbons are shown as a function of the number of reaction runs in Figures 9 and 10 for Pt(111) and ($\sqrt{3}\times\sqrt{3}$)-R30°−Sn/Pt(111), respectively. It is evident in both figures that the most significant decreases in catalytic activities occur in the first reaction run over both surfaces. Over Pt(111), which

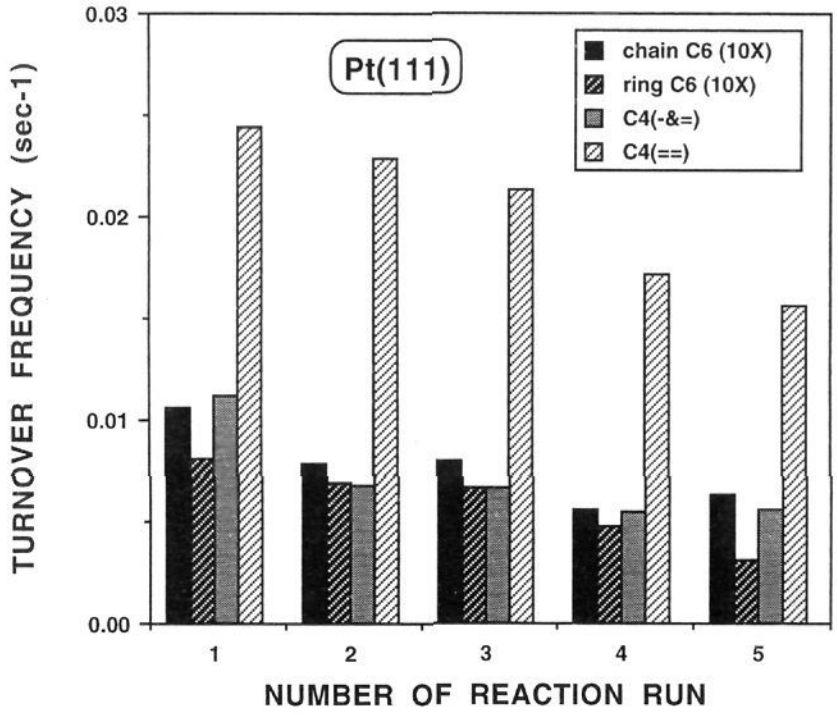

Figure 9. Deactivation of Pt(111) in the di- and trimerization of acetylene.

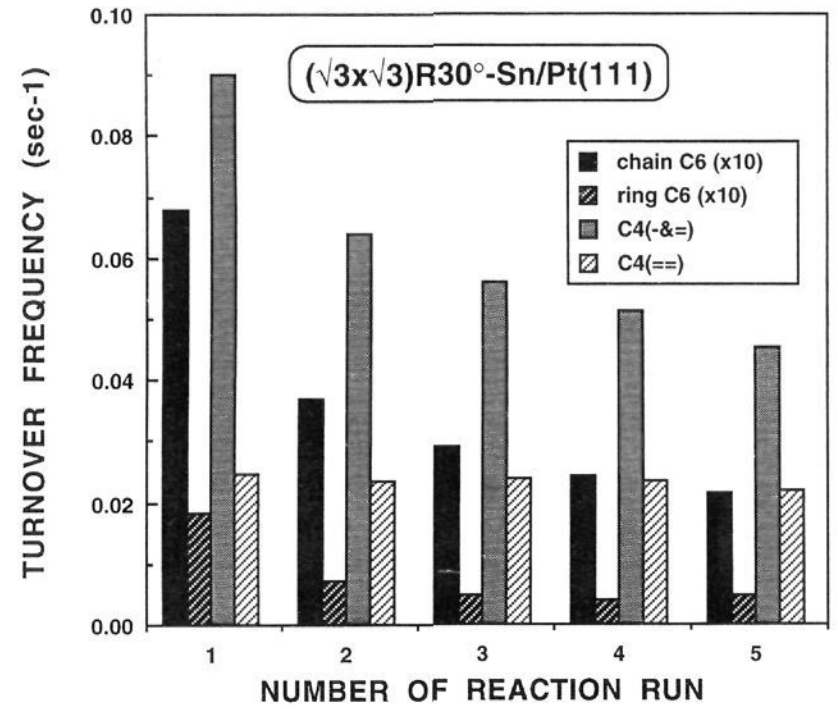

Figure 10. Deactivation of $(\sqrt{3}\times\sqrt{3})R30°-Sn/Pt(111)$ surface alloy in the di- and trimerization of acetylene.

produces butadiene as the main reaction product at 500 K, hardly any change in product selectivities can be observed. A comparison of product selectivities for the first and fifth reaction runs reveals that there is practically no change, only an overall reaction rate decrease. At the $(\sqrt{3}\times\sqrt{3})R30°-Sn/Pt(111)$ surface alloy the dominant hydrocarbon products are $C_{4(-\&=)}$ in each and every reaction run. After the first catalytic run the $C_{4(-\&=)}$, linear, and ring C_6 formation rates drop significantly and they decrease with slower rates during subsequent reaction runs. It is interesting to note that the TOF for butadiene formation is not affected by the overall deactivation of this catalyst. The carbon buildup, shown as carbon Auger signal intensity, as a function of the number of reaction runs is displayed in Figure 11 for both Pt(111) and $(\sqrt{3}\times\sqrt{3})R30°-Sn/Pt(111)$ surfaces. The carbon Auger signal intensity increases linearly with the number of catalytic runs over Pt(111). On the $(\sqrt{3}\times\sqrt{3})R30°-Sn/Pt(111)$ surface alloy the initial carbon buildup is about twice as high as on Pt(111). However, the increase in carbon Auger signal intensity in subsequent reaction runs is much less pronounced for the alloy surface than for Pt(111). The carbon level on $(\sqrt{3}\times\sqrt{3})R30°-Sn/Pt(111)$ is approximately the same after the fourth and fifth catalytic reaction.

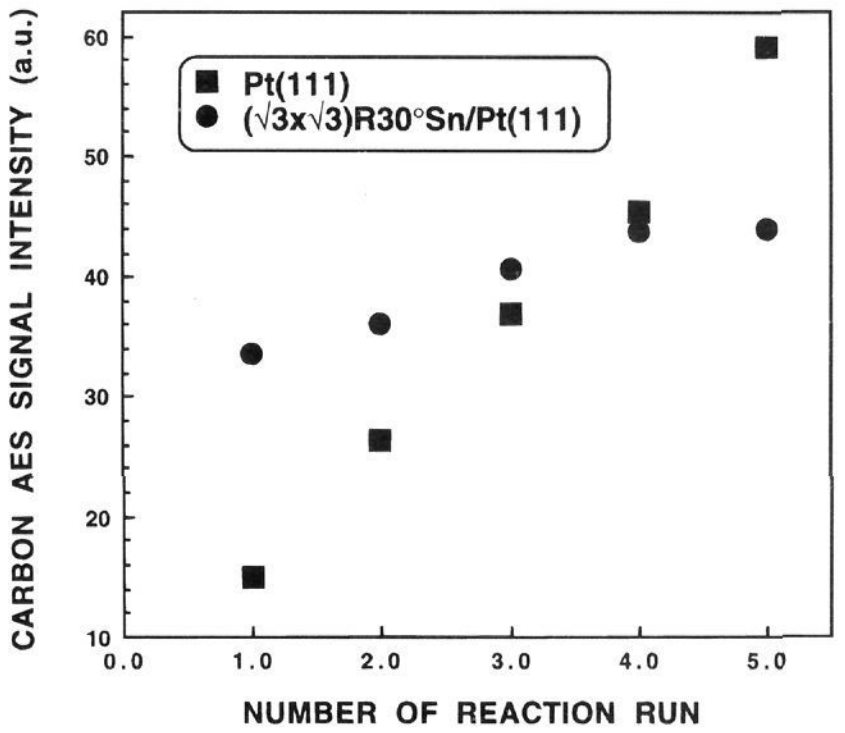

Figure 11. Post reaction carbon coverage on Pt(111) and $(\sqrt{3}\times\sqrt{3})R30°-Sn/Pt(111)$ surfaces during the di- and trimerization of acetylene as a function of batch reaction run.

4. Discussion

The reaction of a $C_2H_2 + H_2$ gas mixture over both Pt(111) and $(\sqrt{3}\times\sqrt{3})R30°-Sn/Pt(111)$ surfaces produced only C_4 and C_6 di- and trimerization hydrocarbon products with no C_3 or C_5 hydrocarbons detected. Depending on the experimental conditions [$P_{H_2}/P_{C_2H_2}$, and T], varying amounts of ethylene were also produced as a direct hydrogenation product of acetylene. These observations are in qualitative agreement with those of Ormerod and Lambert,[23] who studied the cyclotrimerization reaction over silica- and titania-supported Pd catalysts. They observed the formation of C_4 products in addition to benzene in either the presence or the absence of hydrogen in the reactant gas mixture. These results are in contrast to those of Rucker et al.,[18,19] who did not observe any C_4 hydrocarbon product. They reported benzene as the sole hydrocarbon produced under their experimental conditions over single crystal, thin film, and supported Pd catalysts. The formation of butadiene, a C_4 hydrocarbon, was also observed in a UHV study by Xu et al.[27] over Sn/Pt surface alloys in the absence of hydrogen. In our experiments C_4 hydrocarbons were the major components of the product gas mixture and their quantities always exceeded that of C_6 hydrocarbon produced. The experimental conditions applied in this study differed from all of the earlier studies in that the reactant gas mixture contained a majority component of hydrogen (under standard reaction conditions the H_2/C_2H_2 ratio was 10). The use of hydrogen containing reactant gas mixtures under elevated pressure conditions over Pd catalysts was not feasible because of the problem of bulk absorption of hydrogen into Pd. The cyclotrimerization of acetylene proceeds readily over single crystal Pd surfaces in the absence of gas-phase hydrogen, and furthermore, the (111) crystal face was shown to exhibit the highest rate for this reaction. However, at elevated pressures, due to the buildup of carbonaceous deposits which are caused by the decomposition of acetylene, fast deactivation of the catalyst was also observed. In our study we did not see any appreciable activity for either Pt(111) or $(\sqrt{3}\times\sqrt{3})R30°-Sn/Pt(111)$ catalysts in the absence of hydrogen in the reactant gas mixture due to the very fast poisoning of these surfaces. In heterogeneous catalytic systems among the Ni congeners (Pd, Pt), Pd is the only reported one to exhibit high activity in the cyclotrimerization of acetylene in UHV. Complete decomposition of acetylene is the main reaction route over both Ni and Pt catalysts and these catalysts display much

lower activities for cyclotrimerization. Conversely, Cu, which adsorbs acetylene weakly, has shown high activity for the cyclotrimerization of acetylene.[9] The key factors in acetylene cyclotrimerization seem to be the sufficient, but not overly strong, acetylene adsorption and the largely undocumented role of adsorbed hydrogen.

Acetylene has been shown to decompose on clean Pt(111) to produce surface carbon and hydrogen. No benzene desorption is observed under UHV conditions.[27] Acetylene adsorption at the p(2×2)−Sn/Pt(111) surface alloy structure (Θ_{Sn} = 0.25 ML, incorporated) results in the desorption of both C_4 and C_6 hydrocarbons, but there is an appreciable decomposition which is evidenced by the large hydrogen evolution in post-adsorption TDMS. Acetylene reaction chemistry at the ($\sqrt{3}\times\sqrt{3}$)R30°−Sn/Pt(111) surface alloy (Θ_{Sn} = 0.33 ML, incorporated Figure 1) nearly suppresses its total decomposition and results in a significant production of benzene and butadiene. Electronic effects in the thermal desorption and sticking probabilites for these and several other hydrocarbon molecules at Sn/Pt(111) surface alloys have been emphasized by Xu et al.[27] It has been shown that the addition of Sn to transition metal catalysts decreases the bond strength between the hydrocarbon and the metal surface.[27,41,45] This effect is attributed to the marked changes in the valence band structure and the orbitals available for hydrocarbon bonding at these Sn/Pt(111) surface alloys.[46] In UHV studies, Sn decreases the extent of acetylene dehydrogenation with increasing concentration of surface Sn atoms. Acetylene dehydrogenates extensively on Pt(111). At the Sn/Pt surface alloys, acetylene more readily, reversibly adsorbs with the dehydrogenation pathway much less favored.

Benzene and cyclohexane adsorption and desorption measurements at the p(2×2) and ($\sqrt{3}\times\sqrt{3}$)R30°−Sn/Pt(111) surface alloys have been reported by Xu et al.[45] Several important features of the UHV results are relevant to the kinetic study presented here. Benzene adsorption was dramatically decreased in saturation coverage, sticking coefficient, and binding energy at the ($\sqrt{3}\times\sqrt{3}$)R30°−Sn/Pt(111) surface alloy in comparision to Pt(111), and these effects were primarily attributed to steric site-blocking. Cyclohexane adsorption, although also displaying a marked decrease in binding energy at the ($\sqrt{3}\times\sqrt{3}$)R30°−Sn/Pt(111) surface alloy, did not exhibit any significant decrease in either sticking coefficient or saturation coverage. With respect to the kinetic data presented in Figures 2 and 3, the production of benzene displays a dramatic drop between 450 and 500 K at the ($\sqrt{3}\times\sqrt{3}$)R30°−Sn/Pt(111) surface alloy. We suggest that the hydrogenation and decreased energetics of surface binding of alkenes and alkanes[40,45] at the ($\sqrt{3}\times\sqrt{3}$)-R30°−Sn/Pt(111) surface alloy strongly alter the available reaction pathways such that hydrogenation to linear C_4 and C_6 compounds is favored.

The temperature dependences of the formation rates of all C_4 and C_6 hydrocarbons are very similar on Pt(111) and the ($\sqrt{3}\times\sqrt{3}$)R30°−Sn/Pt(111) surface alloy. In the range of 400−480 K all the production rates (TOFs) increase with increasing reaction temperature. In addition, the formation rate of butadiene parallels that of $C_{4(-\&=)}$ and the ring C_6 production rate follows closely that of linear C_6 hydrocarbons. Between 480 and 520 K there is a dramatic change in activity patterns. In particular, over the ($\sqrt{3}\times\sqrt{3}$)R30°−Sn/Pt(111) surface alloy this effect is extremely pronounced. The formation rate of butadiene does not follow that of $C_{4(-\&=)}$ and similarly the ring C_6 formation rate pattern deviates from that of linear C_6 hydrocarbons. The butadiene formation rate drops almost an order of magnitude in this temperature range and the TOF for the production of ring C_6 hydrocarbons decreases by more than an order of magnitude to only trace amounts. It is important to note that the formation rate of ring C_6 hydrocarbons parallels that for butadiene. Above 520 K both butadiene and ring C_6 formation rates are high again and follow the $C_{4(-\&=)}$ and linear C_6 production patterns, respectively. The production rates of $C_{4(-\&=)}$ and linear C_6 hydrocarbons are essentially unchanged over the temperature range where the butadiene and ring C_6 formation rates drop to low values. After the TOFs for butadiene and ring C_6 hydrocarbon formation recover (T > 520 K), the TOFs for all products decrease with increasing temperature. The rather unique activity patterns for butadiene and ring C_6 hydrocarbon formation may be explained on the basis of postreaction AES results shown in Figure 4. There is a low level of carbon buildup even at the lowest reaction temperature of 400 K on both surfaces and the carbon levels are practically unchanged in the temperature interval of 400−480 K. In this temperature range both surfaces are partially covered by carbonaceous deposits, but the carbon levels are low and constant. Between 480 and 520 K, however, the surface carbon levels increase dramatically on both catalysts and then they level off above 520 K and stay constant or increase very slowly. In the small temperature interval of 40 K (480−520 K) there is approximately a 4-fold increase in surface carbon coverage. This rapid carbon accumulation on the surface dramatically suppresses the formation rates of butadiene and ring C_6 hydrocarbons. In contrast, the $C_{4(-\&=)}$ and linear C_6 formation rates do not go through these dramatic changes, and over this temperature region the TOFs for these two product groups are almost constant, with very slow decreases. We suggest that the coupling of two acetylene molecules to produce a metallocyclopentadiene is severely suppressed by the rapid carbon buildup. The fact that the carbon buildup mostly results in the depletion of cyclic intermediates/products suggests that the effect of surface carbon in this temperature range is primarily steric. The propagation of $C_{4(-\&=)}$ and C_6 linear hydrocarbons is not noticeably affected by the carbon buildup.

The mechanistic consequences of these observations are very important in that they imply that the initial coupling of two acetylene molecules can proceed through two different reaction pathways. One pathway involves participation of a metallocyclopentadiene (M-C_4) intermediate and another conceivably involves a linear C_4H_x surface species (or ring opening of the metallocyclopentadiene intermediate). On the clean and partially carbon covered surfaces the probability of proceeding along either pathway is approximately equal or interconversion between possible intermediates is rapid. Through a consecutive acetylene insertion step the metallocyclopentadiene intermediate can produce ring C_6 hydrocarbons while a C_4H_x surface species leads to a linear C_6 hydrocarbon molecule. In the presence of gas phase hydrogen it is possible that not all of the surface metallocyclopentadiene molecules react with a third acetylene molecule to form the ring C_6 hydrocarbons but rather a significant fraction of them hydrogenate off from the catalyst surface as butadiene. It is also possible that this metallocyclopentadiene intermediate becomes further hydrogenated on the surface and forms saturated or olefinic C_4 hydrocarbons and it may contribute to the formation of linear C_6 molecules as well. The activity patterns strongly suggest, however, that the linear C_6 hydrocarbons are formed through a linear C_4H_x surface species while the ring C_6 hydrocarbons are produced via the ring expansion of the metallocyclopentadiene intermediates. The significantly higher formation rates for the C_4 than the C_6

(45) Xu, C.; Tsai, Y.-L.; Koel, B. E. *J. Phys. Chem.* **1994**, *98*, 585.
(46) Paffett, M. T.; Gebhardt, S. C.; Windham, R. G.; Koel, B. E. *Surf. Sci.* **1989**, *223*, 449.

hydrocarbon products also suggest that the hydrogenation of surface C_4 species from the catalyst surface proceeds with higher probability than the insertion of the third acetylene molecule into the metal−C_4 intermediate bond. The observed activity patterns and surface analysis data also suggest that the di- and trimerization of acetylene can proceed with fairly high reaction rate even on heavily carbon covered catalyst surfaces. Lacking vibrational spectroscopic data, we do not know the forms of the carbonaceous deposits on either surface. In a study of acetylene cyclotrimerization over Pd single crystal surfaces Rucker et al.[18] also observed that the reaction proceeded with fairly high efficiency even over catalyst surfaces covered with carbonaceous deposits. They proposed, on the basis of the very low apparent activation energy observed (~2 kcal mol^{-1}), that benzene formation can take place on the ethylidyne overlayer or over other carbonaceous fragments that do not strongly adsorb benzene. The high catalytic activities seen in this study over heavily carbon covered surfaces provide an interesting parallel.

No di- and trimerization product formation was seen over either catalyst surface in the absence of gas-phase hydrogen. This surface carbonaceous layer that rapidly developed entirely eliminated the catalytic activities of these surfaces for the di- and trimerization of acetylene. On the contrary, in the presence of gas-phase hydrogen [with $P_{H_2}/P_{C_2H_2} \geq 2$] both catalyst surfaces showed high activities for C_4 and C_6 hydrocarbon formation, even under experimental conditions when the catalyst surfaces were covered with a significant carbonaceous deposit. This observation suggests that the compositions and reactivities of the surface carbonaceous layers are different under the two reaction conditions (i.e. in the absence and in the presence of gas-phase hydrogen). At elevated acetylene pressures in the absence of hydrogen the most probable process is the complete dehydrogenation of acetylene into surface carbon with increasingly smaller amounts of incorporated hydrogen as the temperature increases. In contrast, the presence of substantial amounts of hydrogen in the gas phase impedes the formation of this more graphitic-like layer and instead produces a carbonaceous layer that contains more incorporated hydrogen. The formation of this hydrogen containing carbonaceous layer on the catalyst surface does not result in the complete loss of catalytic activity for the di- and trimerization of acetylene.

From the activity patterns observed throughout this study the participation of surface CH_y species in the coupling reactions can be eliminated. For these surface species to play a significant role in the chain propagation or ring extension reactions we should have detected C_3 and C_5 hydrocarbons in the product gas mixture. The observed large drop in butadiene and ring C_6 formation rates in the 480−520 K temperature interval may be caused by a loss of hydrogen in the adsorbed C_xH_y and/or from a phase transition of the carbonaceous deposit layer.

Note that at the $(\sqrt{3}\times\sqrt{3})$R30°−Sn/Pt(111) surface alloy the buildup of a carbonaceous surface layer following moderate pressure exposure to acetylene is only partially suppressed. In the UHV study of Xu et al.[27] acetylene decomposes completely to produce surface carbon on the Pt(111) surface, but over the $(\sqrt{3}\times\sqrt{3})$R30°−Sn/Pt(111) surface 35% of a saturated monolayer dehydrogenates and the acetylene either desorbs or participates in the di- and trimerization reactions. These reactions were performed in the absence of added or adsorbed hydrogen. At elevated pressures, Pt(111), which was shown to be inactive for the di- and trimerization in UHV, is only about 4−5 times less active than the $(\sqrt{3}\times\sqrt{3})$R30°−Sn/Pt(111) surface, which was seen to be orders of magnitude more active in the UHV studies.

The hydrogen partial pressure dependences of C_4 and C_6 product formation rates exhibit very similar patterns on the two surfaces studied. At low hydrogen partial pressures (5−10 Torr) the rates for each and every product formed are first order in hydrogen pressure. In this hydrogen pressure region the postreaction Auger analysis showed the presence of a constant, high level of a carbonaceous layer on the catalyst surfaces. The formation rates of butadiene and ring C_6 hydrocarbons reached maxima at $P_{H_2} \sim 10$ Torr on both surfaces and then at higher hydrogen pressures they decreased gradually with increasing hydrogen pressure. The TOFs for butadiene and ring C_6 formation parallel each other in the entire hydrogen pressure interval studied. This suggests that their formation proceeds through a common surface intermediate species, most probably through a metallocyclopentadiene. One of the mechanisms suggests that benzene is formed via the addition of an acetylene molecule to the metallocyclopentadiene surface species while another proposes the coupling of two surface metallocyclopentadiene species to form a cyclooctatetraene entity which subsequently decomposes into a benzene and an acetylene molecule. The fact that we could detect neither cyclooctatetraene nor other C_8 hydrocarbons in the product mixture under any of the experimental conditions studied supports the first reaction pathway for ring C_6 formation on these surfaces and under the given reaction conditions. We suggest that the formation of ring C_6 hydrocarbons proceeds through a butadiene intermediate which is present on the surface as a metallocyclopentadiene based on the very strong correspondence between the butadiene and ring C_6 formation rates throughout this study.

Increasing the hydrogen partial pressure above 10 Torr results only in subtle changes in the $C_{4(-\&=)}$ and linear C_6 hydrocarbon formation rates. Over the Pt(111) surface their formation rates are constant at $P_{H_2} > 20$ Torr while on the $(\sqrt{3}\times\sqrt{3})$R30°−Sn/Pt(111) surface alloy they pass through maxima at ~15 Torr of hydrogen partial pressure and then they decrease slowly. However, the decrease in turnover frequencies for $C_{4(-\&=)}$ and linear C_6 productions is not nearly as pronounced as is seen for either the butadiene or ring C_6 formation. Since the di- and trimerization of acetylene can take place readily over the carbonaceous layer covered surfaces, the sharp decrease in the formation rates of butadiene and ring C_6 hydrocarbons corresponds to the sudden fall in the surface carbon level on both catalyst surfaces. Above 20 Torr of hydrogen pressure the carbon levels are constant on both surfaces with Pt(111) exhibiting a somewhat higher carbonaceous species concentration between 20 and 100 Torr. The sharp decreases in both butadiene and ring C_6 hydrocarbon formation rates suggest that the rate of formation and/or the stability of the common intermediate in butadiene and ring C_6 formation (presumably the metallocyclopentadiene) drastically decreases with increasing hydrogen pressure above 20 Torr. The unsaturated C_4 intermediates are observed to hydrogenate at higher hydrogen pressures and favor the formation of C_6 hydrocarbons other than cyclic C_6 molecules.

The extent of acetylene hydrogenation to ethylene should also be mentioned. At the highest hydrogen pressures studied the major product C_2 hydrocarbon present after catalytic reaction is ethylene. In our related work[34] on ethylene/H_2 reactions over the same catalyst surfaces ethylene does not produce either butadiene or ring C_6 hydrocarbons, but rather only $C_{4(-\&=)}$ and trace amounts of linear C_6 hydrocarbons. Both Pt(111) and the $(\sqrt{3}\times\sqrt{3})$R30°−Sn/Pt(111) surfaces produce C_4 and C_6 linear hydrocarbons with high reaction rates even at high hydrogen pressures when acetylene is used as the reactant. This suggests that the insertion of an acetylene molecule into the surface−

C_2H_y and surface$-C_4H_z$ bonds to produce linear products is not diminished by a high H_{ads} concentration.

The formation rates for $C_{4(-\&=)}$ and linear C_6 hydrocarbons increase monotonically with increasing acetylene partial pressure over the entire acetylene pressure range studied. In the low acetylene partial pressure interval of 0.5−1.5 Torr the TOFs for both butadiene and ring C_6 hydrocarbons increase very rapidly. Above 1.5 Torr, the rates continue to increase monotonically but at decreased rates. The low butadiene and ring C_6 formation rates observed at high $P_{H_2}/P_{C_2H_2}$ ratios can be understood on the basis of hydrogenation reactions preferentially producing linear saturated products at high hydrogen partial pressures. The formation rates of all hydrocarbons are positive order in acetylene pressure, although the TOFs for butadiene and ring C_6 production are more positive than those seen for $C_{4(-\&=)}$ and linear C_6 hydrocarbons. This observation demonstrates that with increasing acetylene/hydrogen ratios the formation rates and stabilities of surface intermediates responsible for the production of ring C_6 hydrocarbons increase. The TOFs for ring C_6 and linear C_6 hydrocarbons increase faster than those for butadiene and $C_{4(-\&=)}$, respectively, with increasing acetylene partial pressure. This suggests that as the acetylene partial pressure increases, an increasing fraction of metallocyclopentadiene transforms into ring C_6 hydrocarbons and an increasing amount of acetylene is inserted into the surface$-C_4H_x$ bond producing more linear C_6 hydrocarbons.

The deactivation patterns over the two surfaces are not substantially different. On the Pt(111) surface at 500 K (Figure 2), butadiene is produced with the highest rate and it remains the most dominant product even at very high carbonaceous deposit concentrations. The changes in ring C_6 hydrocarbon formation rates follow very closely that of butadiene. With increasing number of reaction runs the overall catalytic activity of Pt(111) decreases but the product selectivities remain practically unchanged. This suggests that under a given set of reaction conditions the deposition of carbonaceous residues results only in a decrease of the number of catalytically active sites but does not significantly modify the nature of the active sites and, therefore, does not change the product selectivities. Even after the fifth reaction run substantial amounts of C_4 and C_6 di- and trimerization products can be obtained although the catalyst surface is very heavily covered with carbonaceous deposits. The same is true for the $(\sqrt{3}\times\sqrt{3})$R30°−Sn/Pt(111) surface alloy as well. The overall activity of this catalyst decreases with the number of reaction runs but there is only a slight change in product selectivities. The only noticeable difference between the two surfaces is that over the alloy surface the TOFs for butadiene formation are unchanged with the number of reaction runs. On the $(\sqrt{3}\times\sqrt{3})$R30°−Sn/Pt(111) surface the high level of carbonaceous deposits does not suppress completely the catalytic activity (i.e., the di- and trimerization reaction of acetylene proceeds in the presence of a significant carbonaceous overlayer). The carbonaceous layer covered surfaces show appreciable catalytic activity as long as a significant amount of hydrogen is present in reaction conditions (i.e. C_xH_y species formed at the surface). As the reaction proceeds at higher T or lower P_{H_2} the carbonaceous layer may lose hydrogen to form more a graphite-like carbon that acts as a poison for the di- and trimerization reactions. Additional vibrational spectroscopic and STM studies could substantiate these proposals.

In summary, both Pt(111) and $(\sqrt{3}\times\sqrt{3})$R30°−Sn/Pt(111) model catalysts show high activity for the di- and trimerizarion of actylene under elevated pressure conditions. Only C_4 and C_6 di- and trimerization products were detected, with no C_3 or C_5 hydrocarbon formation observed. Among the C_6 products both aliphatic and cyclic hydrocarbons were seen. Under our experimental conditions the reaction rates for C_4 hydrocarbon formation were always approximately an order of magnitude higher than that for C_6 hydrocarbons. Besides the di- and trimerization products, ethylene formation was also observed as a result of the direct hydrogenation of acetylene in the presence of hydrogen. The $(\sqrt{3}\times\sqrt{3})$R30°−Sn/Pt(111) surface alloy proved to be ~4−5 times more active in the acetylene di- and trimerization than the clean Pt(111). The results of this study strongly suggest that the formation of cyclic hydrocarbons proceeds through a common metallocyclopentadiene intermediate which can either be hydrogenated off from the surface as butadiene or react with another acetylene molecule to produce cyclic C_6 products. Postreaction surface analysis results suggest that the reaction readily proceeds even over surfaces with a heavy carbonaceous deposit although the catalysts lose their activities at sufficiently high Θ_C.

Acknowledgment. It is a pleasure to acknowledge a critical reading of the manuscript by Prof. Bruce E. Koel, Chemistry Department, University of Southern California.

JA941416D